The Electrical Resistivity of Ultra-Thin Copper Films

Ernst Schmiedl[a], Peter Wissmann[a], and Hans-Ulrich Finzel[b]

[a] Institut für Physikalische und Theoretische Chemie, Universität Erlangen-Nürnberg, Germany
[b] FB Chemie der Hochschule Niederrhein, Adlerstr. 32, D-47798 Krefeld, Germany

Reprint requests to H.-U. F.; E-mail: hans-ulrich.finzel@hsnr.de

Z. Naturforsch. **63a,** 739 – 744 (2008); received May 16, 2008

The resistivity of ultra-thin metal films is much higher than theoretically predicted by the scattering hypothesis. The effect is discussed with respect to the variation of film thickness for copper films deposited under ultra-high vacuum conditions on glass substrates. The interpretation on the basis of a statistical model leads to reasonable results even when the variation of temperature is included into consideration. Additional information is obtained from photoelectric and field effect measurements.

Key words: Ultra-Thin Films; Electrical Resistivity.

1. Introduction

The electrical properties of homogeneous metal films can be interpreted on the basis of the scattering hypothesis. Quantitatively [1]

$$\rho = \rho_0 \left(1 + \frac{C}{d}\right) \qquad (1)$$

is valid for the description of the dependence of the electrical resistivity ρ on the film thickness d. Here, ρ_0 is the resistivity of bulk material, with the same lattice defect density as the films have themselves, and C is the scattering constant. Many attempts have been made, however, to provide a proper extension of the theory also to the ultra-thin region by considering electron tunneling phenomena [2, 3], Monte-Carlo simulations [4, 5] or rescaling theories [6, 7]. We prefer a statistical model which has already been successfully applied to ultra-thin silver [8] and gold [9] films. In this model, film deposition and crystal growth are simulated by a Monte-Carlo method, and the development of closed current paths is analyzed using classical network analysis [10].

The model is based on the assumption that copper islands are formed which are connected by highly ohmic bridges. The main aim of the present study is to check whether this model can satisfactorily describe the thickness dependence of the electrical resistivity and the temperature coefficient of resistivity (TCR) of thin copper films. Information on the film structure is derived from photoelectric and field effect measurements. The data widely agree with the excellent survey of Chopra [11] concerning the crystal growth of thin metal films on glass.

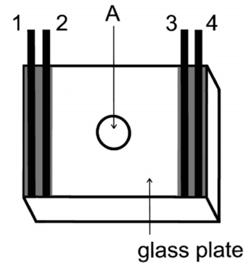

Fig. 1. Schematics of the four-pole contacts for glass substrates. A indicates the illuminated spot, the shaded area represents an 1 μm thick Mo contact layer predeposited in the UHV.

2. Thickness Dependence of the Film Resistivity

The schematics of the glass substrates used in the present investigation is shown in Figure 1. The substrate was either a glass plate (Schott no. 8487) with four molten-in tungsten terminals serving as electrical contacts or a spherical glass bulb with two ring-shaped platinum electrodes at the inner part of the wall [8]. Film thickness was recorded in situ by a vibrating quartz monitor. Details of the ultra-high-vacuum (UHV) apparatus, the resistivity as well as the thickness measurements and the film illumination are described elsewhere [8, 12]. Figure 2 shows the thickness dependence of the resistivity of copper films. ρ

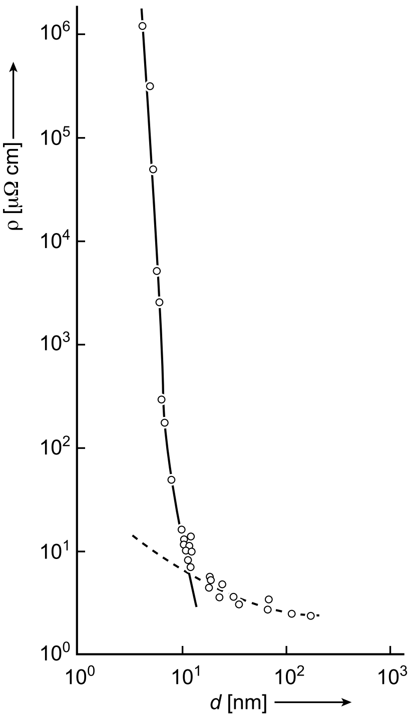

Fig. 2. Thickness dependence of the resistivity of evaporated copper films at 293 K. (○) Experimental data; (—) calculated according to the statistical model [10]; (- - -) calculated on the basis of (1). For the fit parameters see Table 1.

was calculated from the measured resistance R according to [12].

$$\rho = \frac{Rd}{F}, \tag{2}$$

where F is a dimensionless geometric factor. The doubly logarithmic plot of Fig. 2 contains experimental data along with theoretical curves calculated with the help of (1) or in the framework of the statistical model [10]. One immediately recognizes that only the statistical model can describe the experimental data in the ultra-thin region.

This model starts by dividing the film in rectangular cells, occupying them statistically with the help of a random generator, and performing a classical network analysis under suitable assumptions [10]. By the diagonal connections between the cells also the short circuiting through highly ohmic bridges [13] or tunneling barriers [2, 3] can be included into the calculation.

Characteristic parameters of the model are d_0 and $\rho_0{}^+$. d_0 is the thickness, where all cells are uniquely occupied, and $\rho_0{}^+$ is the corresponding resistivity. Both quantities can be read out from the solid curve in Fig. 2; the results of the fit are listed in Table 1 along with the scattering constant C. The d^{-3} law describing roughness effects [8] does not play an important role in the present case. Moreover, scaling laws [7] or a d^{-2} dependence [14] are found to be ineffective in explaining the measured data.

d_0 [nm]	10
$\rho_0{}^+$ [$\mu\Omega$ cm]	18
ρ_0 [$\mu\Omega$ cm]	2.2
C [nm]	20

Table 1. Fit parameters for the theoretical curves in Figure 2.

3. The Absolute Temperature Coefficient of Resistivity (ATCR)

For selected films, the deposition process was interrupted at several thicknesses, and the film was then cooled to 77 K in order to determine the ATCR values β [12, 15] according to

$$\beta = \frac{\rho_{293\,\mathrm{K}} - \rho_{77\,\mathrm{K}}}{293\,\mathrm{K} - 77\,\mathrm{K}}. \tag{3}$$

Figure 3 shows the data points in a plot β versus film thickness d. The ATCR values are strongly negative for ultra-thin films, then pass through a steep maximum, and finally approach the well-known bulk value β_0. This behaviour can again be interpreted with the help of the statistical model by attributing a negative sign

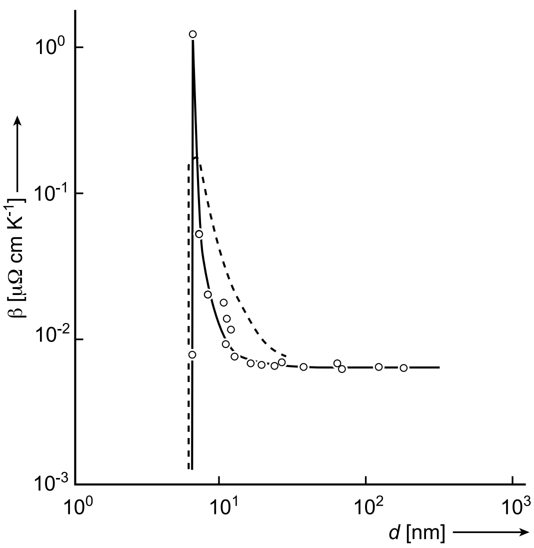

Fig. 3. Absolute temperature coefficient of resistivity (ATCR) of evaporated copper films in dependence on the film thickness. (○) Experimental data; (- - -) calculated according to the statistical model [13]; for details see text.

and a variable weight factor γ to the contribution of the highly ohmic bridges [13] which are represented by the transition between two diagonally neighbouring cells. For $\gamma = 1000$, $\beta_0 \approx 7 \cdot 10^{-3}$ $\mu\Omega\,\text{cm}\,\text{K}^{-1}$ [16] and d_0 = 10 nm (refer to Table 1) one obtains the dashed theoretical curve in Figure 3. General features of the experimental data are represented by this curve. A better coincidence, however, would be expected if the calculation is based on still higher γ values [13].

An influence of thermally induced strains [17], which can be traced back to the differing thermal expansion coefficients of film and glass substrate, does not play an important role in explaining the resistivity behaviour. Such an effect should cause the β values to deviate from the bulk value even for thicker films, in contradiction to the experimental evidence.

4. Photoelectric Measurements

We now turn to photoelectric measurements to get additional information on the structure and particularly on the island formation in ultra-thin copper films. The illumination of the film substrate is schematically illustrated in Figure 1. The light of a high-pressure mercury lamp enters the cell by quartz windows, details are described elsewhere [12]. The emitted electrons are collected by a suitable electrode to form the photocurrent. The evaluation is based on Fowler's theory [18] which predicts a linear relationship between the square root of the photoelectric yield, $\sqrt{I}$, and the light frequency, ν, in a medium frequency range, i. e.,

$$\sqrt{I} \sim (\nu - \nu_0). \tag{4}$$

The extrapolation to $\sqrt{I} \to 0$ leads to

$$\nu = \nu_0 = \frac{e}{h}\phi, \tag{5}$$

where h is Planck's constant and $e\phi$ the work function [19, 12]. The usual behaviour of thin films is a quick approach to the saturation value of the photocurrent during illumination. Ultra-thin films, on the contrary, can be characterized by a strong time dependence of the photocurrent as shown in Figure 4.

After switching on the light, the photocurrent steeply increases to a sharp maximum I_M, and then decreases steadily towards a constant residual value I_s. Both the maximum and the saturation value obey to the linear relationship of (4). A corresponding plot of $\sqrt{I}$ versus the energy $h\nu$ is shown in Fig. 5; the extrapolation to $\sqrt{I} \to 0$ yields $e\phi = 4.56$ eV for both curves.

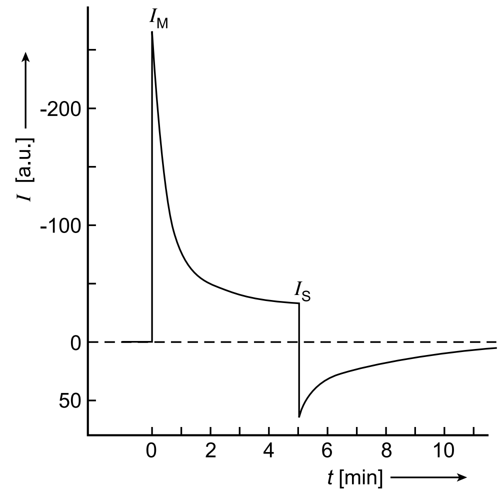

Fig. 4. Photoelectric yield I in dependence on time t for a 6.8 nm thick copper film at $\lambda = 248.2$ nm.

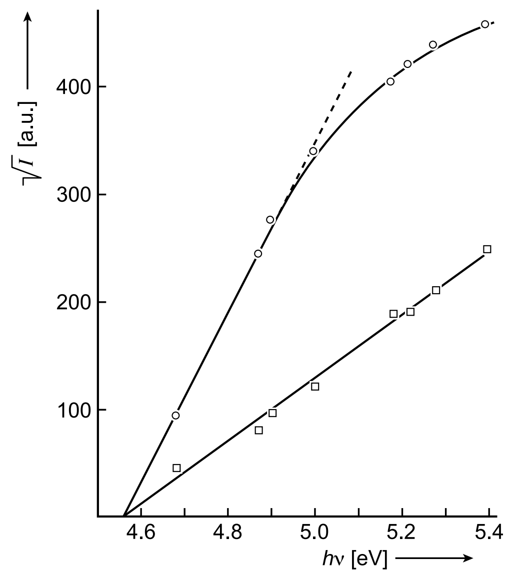

Fig. 5. Fowler plot for the maximum I_M (○) as well as for the saturation value I_s (□) for the film of Figure 4.

This value roughly corresponds to the data published in [20, 21] for thin copper films; no size dependence can be detected. The flattening of the curves at higher frequencies has also been observed by Berglund and Spicer [22] who attributed this to a decreasing escape probability of the photoelectrons.

After switching off the light an inverse current is observed in Fig. 4 which slowly approaches to zero. A strong scattering of the amount of the inverse currents and even a change of their signs are typical for ultra-thin films.

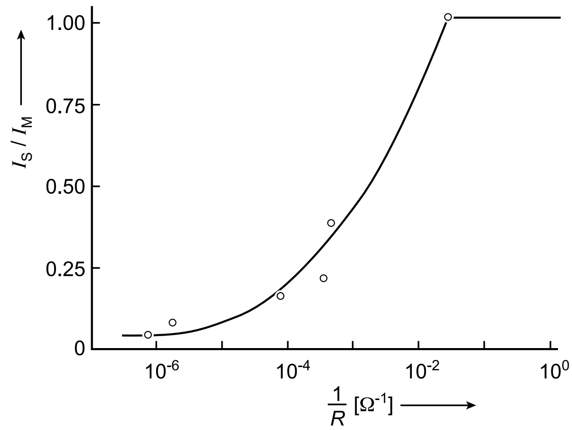

Fig. 6. Relation between I_s/I_M and the reciprocal resistance $1/R$. For details see text.

In order to interpret the kinetics of the curves of Fig. 4 we look at the ratio I_s/I_M. This quantity is plotted in Fig. 6 versus $1/R$ which represents a qualitative measure of the film thickness according to (2). The curve steadily increases up to the bulk value of (1). We conclude that the statistical model [8] finds an additional justification here. Some metallic islands are connected by low-ohmic bridges, others remain more or less isolated. Both island types contribute to the photocurrent after switching on the illumination. The isolated islands, however, quickly reduce their electron storage, so that the photoelectric yield is reduced to the portion originating from connected islands. Hence small I_s/I_M values are typical for large portions of isolated islands, high I_s/I_M values approach the bulk properties where the whole film area is electrically connected and contributes to the photoelectric yield.

We should mention that many checks have reconfirmed the missing of any detectable influence of the illumination on the film resistivity. Probably, the illumination power of our high-pressure mercury lamps is not sufficient to produce an efficient photoionization of the bridge atoms which govern the high-ohmic conductivity.

5. The Properties of Ultra-Thin Copper Films

Now the question arises whether the bridges can be represented by tunneling electrons [23] or by short metallic nanobridges [24]. In order to put a new light on this problem we have investigated the influence of time, voltage, and external electric fields on the resistivity of films with $R > 100\ \text{k}\Omega$, i. e. films with a rather high amount of isolated islands, where the high-ohmic bridges should particularly strongly dominate the conduction mechanism.

5.1. Kinetics of the Resistivity

The resistivity of ultra-thin films varies with time as mentioned in previous papers [8, 12]. Figure 7 shows a typical example. During deposition the resistivity steeply decreases. After stopping the deposition, an increase in resistivity is observed with time constants in the minute range. Obviously, coagulation of copper with an enhanced formation of isolated islands becomes effective. Similar results can be expected on the basis of actual results of various groups [25, 26] due to a current-induced embrittlement and breaking of the bridges. In particular, extremely thin bridges loose their conducting ability, thus enhancing the resistivity.

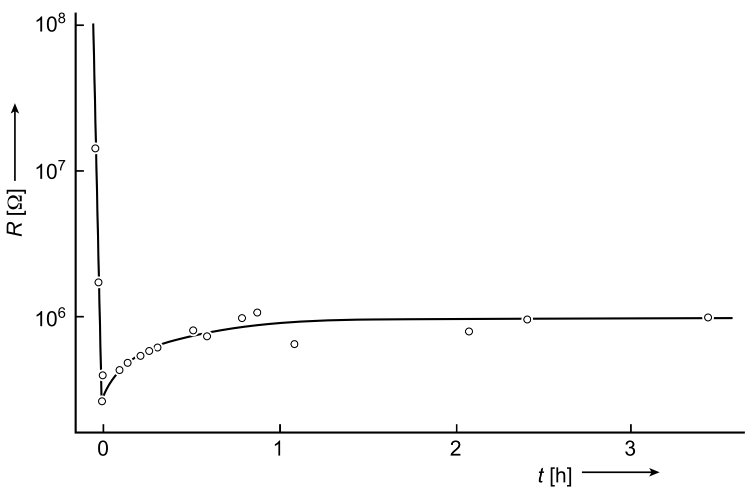

Fig. 7. Time dependence of the resistance R of a 6.8 nm thick copper film at 293 K.

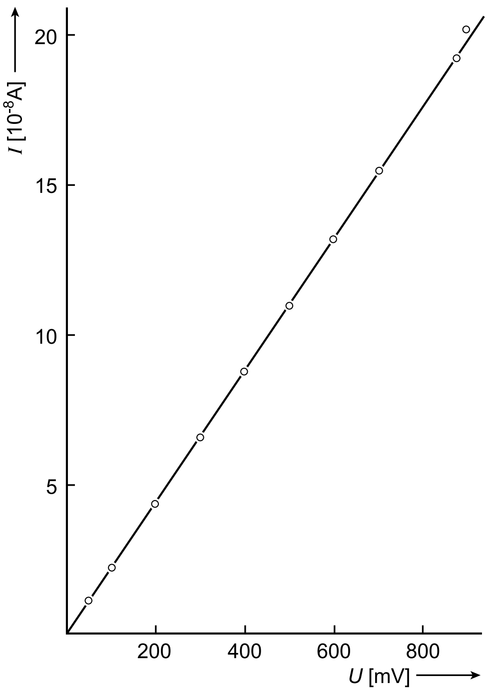

Fig. 8. IV characteristics for a 6.8 nm thick copper film at 293 K.

The influence of current heating seems to be of minor importance even at ambient temperature [27].

5.2. IV Characteristics

We have also recorded IV characteristics in order to improve the ohmic behaviour of the films. Figure 8 represents a corresponding curve obtained at 293 K. No deviations from linearity can be found in the current range investigated here, contrary to the expectation for a dominating tunneling mechanism [11, 28].

5.3. Field Effect Measurements

Further information on the physical properties of the bridges is obtained from field effect measurements. Details on the experimental arrangement are described in [29, 12]. By means of a suitably dimensioned field electrode-influenced charges ΔQ are induced which vary the surface conductivity $\Delta\sigma$ in a characteristic manner [30]. A typical dependence measured for a 660 kΩ copper film is shown in Fig. 9; the curve passes through a minimum at $\Delta Q_{\rm min} = 3.6 \cdot 10^{-9}$ As/cm^2. The signal intensity becomes smaller and no minimum can be realized in the case of thicker films. Field effect curves as shown in Fig. 9, however, have been also described for ultra-thin films of nickel [29]. So the change of the sign of $\Delta\sigma/\Delta Q$ represents a certain universal character and resembles to the case of n-conducting semiconductors, where a formal evaluation leads to carrier densities reduced by orders of magnitude compared to the bulk value [12]. We conclude that most likely the high-ohmic brigdes consist of a chain of single copper atoms which enable the electrons to tunnel through. The tunneling probability is then modified by the field-induced charging [31, 32], which results in a rather strong change in the surface conductivity $\Delta\sigma$.

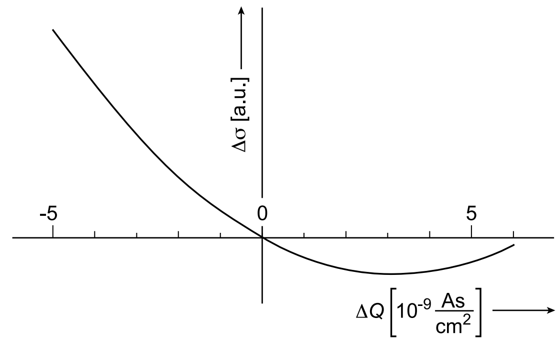

Fig. 9. Schematical field effect curve for an ultra-thin copper film with a resistance of 660 kΩ.

6. Discussion and Conclusions

The thickness dependence of the resistivity and the ATCR of ultra-thin polycrystalline films can be satisfactorily interpreted with the help of the statistical model. Hence the basic assumptions of this model seem to be justified. Evidently, a reduction of the geometric cross-section for the conduction paths and the island formation are responsible for the strong increase of resistivity with decreasing thickness.

The photoelectrical measurements elucidate that large isolated areas show the normal band structure of copper but do not contribute to the conductivity. Here we may state that the exact amount of islands strongly depends on the structure, chemistry, and cleanness of the substrates under investigation. Excellent vacuum conditions during the deposition process are a prerequisite for reproducible results.

A remaining question of the interpretation, however, is the physical character of the "high-ohmic bridges" forcing the ATCR values to change their signs for thicknesses lower than d_0. Here, a tunnel mechanism or short metallic nanobridges are discussed in literature. Probably, the bridges can be represented by a chain of single atoms. Arguments for such a mechanism can be derived from field effect measurements. The charging of the metal atoms influences their conductance as well as the tunneling probability of the electrons. The dominating parameter is the distance between the atoms which provides a smooth transition from tunneling to contact regime [33]. Less importance must be attributed to the chemical interaction of the atoms with the underlying glass substrate because of the comparability of the results obtained for nickel and copper.

[1] P. Wissmann, Springer Tracts Mod. Phys. **77**, 1 (1975).

[2] R. M. Hill and T. J. Coutts, Thin Solid Films **42**, 201 (1977).

[3] J. D. Benjamin, C. J. Adkins, and J. E. Van Cleve, J. Phys. C **17**, 599 (1984).

[4] T. J. Coutts and B. Hopewell, Thin Solid Films **9**, 37 (1971).

[5] Z. H. Meiksin, A. Sedehi, and J. R. Blanchere, Thin Solid Films **115**, 33 (1984).

[6] J. G. Zabolitzky, Phys. Rev. B **30**, 4077 (1984).

[7] J. A. J. Lourens, S. Arajs, H. F. Helbig, E.-S. A. Mehanna, and L. Cheriet, Phys. Rev. B **37**, 5423 (1988).

[8] D. Dayal, H.-U. Finzel, and P. Wissmann, in: Thin Metal Films and Gas Chemisorption (Ed. P. Wissmann), Elsevier, Amsterdam 1987, p. 53.

[9] D. Dayal and P. Wissmann, Vakuum-Technik **38**, 121 (1989).

[10] H.-U. Finzel and P. Wissmann, Z. Naturforsch. **40a**, 161 (1985).

[11] K. L. Chopra, Thin Film Phenomena, Mc Graw-Hill, New York 1969.

[12] P. Wissmann and H.-U. Finzel, Springer Tracts Mod. Phys. **223**, (2007).

[13] H.-U. Finzel and P. Wissmann Z. Naturforsch. **40a**, 1066 (1985).

[14] Z. Tesanovic, M. V. Jaric, and S. Maekawa, Phys. Rev. Lett. **57**, 2760 (1986).

[15] H.-U. Finzel, D. Lazarov, M. Rauh, and P. Wissmann, Verhandl. Ger. Phys. Soc. VI **25**, 657 (1990).

[16] G. Wedler and W. Wiebauer, Thin Solid Films **28**, 65 (1975).

[17] R.W. Vook, in: Epitaxial Growth, Part A (Ed. J.W. Matthews), Academic Press, London 1975.

[18] R. H. Fowler, Phys. Rev. **38**, 45 (1933).

[19] E. Schmiedl and P. Wissmann, Vakuum-Technik **33**, 78 (1984).

[20] D. Dayal, Thesis, University Erlangen-Nürnberg, Germany 1976.

[21] H. Buck, Thesis, University Erlangen-Nürnberg, Germany 1987.

[22] C. N. Berglund and W. A. Spicer, Phys. Rev. **136A**, 1044 (1964).

[23] C. A. Neugebauer and M. B. Webb, J. Appl. Phys. **33**, 74 (1962).

[24] H. B. Weber, R. Häussler, H. v. Löhneysen, and J. Kroha, Phys. Rev. B **63**, 165426 (2001).

[25] T. N. Todorov, J. Hoeekstra, and A. P. Sutton, Phys. Rev. Lett. **86**, 3606 (2001).

[26] A. Fujii, M. Tsutsui, S. Kurokawa, and A. Sakai, Phys. Rev. B **72**, 045407 (2005).

[27] Z. Yang, M. Chshiev, M. Zwolak, Y.-C. Chen, and M. di Ventra, Phys. Rev. B **71**, 041402 (2005).

[28] C. Kergueris, J. P. Bourgoin, S. Palacin, D. Esteve, C. Urbina, M. Magoga, and C. Joachim, Phys. Rev. B **59**, 12505 (1999).

[29] H.-U. Finzel and P. Wissmann, Surface Sci. **86**, 83 (1979).

[30] W. Mönch, Semiconductor Surfaces and Interfaces, Springer, Berlin 1993.

[31] K. W. Lehnert, B. A. Turek, K. Bladh, L. F. Spietz, D. Gunnarson, P. Delsing, and R. J. Schoelkopf, Phys. Rev. Lett. **91**, 106801 (2003).

[32] T. Anderson, Phys. Rep. **394**, 157 (2004).

[33] L. Limot, J. Kröger, R. Berndt, A. Garcia-Lekue, and W. A. Hofer, Phys. Rev. Lett. **94**, 126102 (2005).